Sururi *et al.*
Future Journal of Pharmaceutical Sciences (2023) 9:115
https://doi.org/10.1186/s43094-023-00563-4

Future Journal of Pharmaceutical Sciences

RESEARCH Open Access

GC–MS and ADME profile analysis of *Carcinoscorpius rotundicauda* bioactive compounds and their potential as COVID-19 antiviral

Ahmad Misbakhus Sururi[1], Dwi Anggorowati Rahayu[2*], Martina Kurnia Rohma[3], Maftukhatul Faizah[4], Elsa Aulia Vebianawati[4] and Mia Savita[4]

Abstract

Background *Carcinoscorpius rotundicauda* is a species of horseshoe crab that is rarely studied. This animal is often used as part of the blood as a medical sterilization material. This study aims to identify the content of bioactive compounds and their bioactivity as an antiviral for COVID-19. The stages of this research include extraction, GC–MS analysis, molecular docking analysis, and ADME analysis.

Results The results showed that in the ethyl acetate extract of the meat, there were 13 bioactive compounds with dominant compound which is propanoic acid (32.15%). Based on molecular docking, one potential compound was found as an antiviral for COVID-19 ACE2, $3CL^{pro}$, and RdRp inhibitor, namely 2-methyl-5-(4′-methyl phenyl) sulfonyl-4-nitroimidazole. The druglikeness and ADME compound profile shows support as an excellent oral drug compound.

Conclusions *Carcinoscorpius rotundicauda* has potential as an inhibitor of ACE2, RdRp, and $3CL^{pro}$ receptor as an anti-SARS-CoV-2. Further research, such as in vitro and in vivo, is still needed to develop its potential as a COVID-19 antiviral.

Keywords Antiviral, COVID-19, Inhibitor, Drug candidate

Background

Mimi Mintuna (horseshoe crab) is one of the marine arthropods known as living fossils with habitat characteristics in shallow waters. There are currently only four species of Mimi Mintuna in the world: *Limulus polyphemus, Tachypleus gigas, Tachypleus tridentatus*, and *Carcinoscorpius rotundicauda*. The status of *L. polyphemus* and *T. tridentatus* is included as threatened species, while the species *C. rotundicauda* and *T. gigas* are included as having data deficiencies [1, 2]. Due to the habitat degradation of Mimi Mintuna, it faces a high risk of extinction in India, Hong Kong, and Singapore, among other places, whereas the distribution of other species is ambiguous, resulting in a

*Correspondence:
Dwi Anggorowati Rahayu
dwirahayu@unesa.ac.id
[1] Department of Chemistry, Faculty of Mathematics and Natural Science, Universitas Negeri Surabaya, Surabaya, East Java, Indonesia
[2] Department of Biology, Faculty of Mathematics and Natural Science, Universitas Negeri Surabaya, Surabaya, East Java, Indonesia
[3] Department of Pharmacy, Universitas Anwar Medika, Sidoarjo, East Java, Indonesia
[4] Department of Biology Education, Faculty of Mathematics and Natural Science, Universitas Negeri Surabaya, Surabaya, East Java, Indonesia

data deficiency [3–6]. *C. rotundicauda* is a common species in Indonesia that is infrequently utilized. Its sole application is as a remedy for convulsions, also known as rituals to exorcise evil spirits [7].

The existence of these arthropods is still far from primary research studies. The uniqueness of Mimi Mintuna is that her blood does not contain hemoglobin but hemocyanin in the form of copper. The content in the blue blood of these animals provides the only natural source in the form of Limulus amebocyte lysate, a substance that can detect endotoxins, a toxic substance in human blood [8, 9]. Because of its antimicrobial activity, part of the blood tests the sterility of drugs or vaccines [10]. Research on *C. rotundicauda* found that its meat contains terpenoids and steroids. In addition, the plasma has antibacterial activity against *Staphylococcus aureus* and *Bacillus* bacteria [11]. Even so, until now, the research results related to the content of bioactive compounds in *C. rotundicauda* meat have not been published. Bioactive compounds from animals have good effectiveness but minor side effects. Drug compounds that have an activity to inhibit target proteins in viruses are called inhibitors [6, 12].

Three well-known diseases caused by coronaviruses include severe acute respiratory syndrome (SARS), Middle East respiratory syndrome (MERS), and coronavirus disease (COVID-19), which emerged in the twenty-first century and are caused by various coronaviruses (CoVs) [13]. All of these viruses are thought to originate from bats and are transmitted to humans through intermediaries. SARS-CoV-1 and SARS-CoV-2 cause COVID-19 disease, which shares about 80% similarity from the same genome; thus, CoV is included in SARS [14]. This virus enters the body using its spike glycoprotein, which binds to the human body's angiotensin-converting enzyme 2 (ACE2) receptor as a host cell [15]. Furthermore, this virus will replicate with the help of 3C-like protease ($3CL^{pro}$) and RNA-dependent-RNA-polymerase (RdRp) enzymes. $3CL^{pro}$ will help the dimerization process to form other enzymes in the replication process [16], while RdRp will help catalyze the RNA strand of this virus [17]. So a suitable inhibitor is needed to block these three receptors so that SARS-CoV-2 infection can be inhibited. Based on this description, this study has several objectives, including identifying bioactive compounds in *C. rotundicauda* meat and their bioactivity as an antiviral for COVID-19. The present study aims to explore the potential of Mimi Mintuna, an indigenous Indonesian plant, as a natural constituent in the pharmaceutical industry, specifically as a potential candidate for antiviral medications targeting COVID-19.

Results

GC–MS analysis

The results of the GC–MS analysis of the ethyl acetate extract from *C. rotundicauda* meat are given in Fig. 1 and Table 1. There are 13 bioactive compounds in the ethyl acetate extract, with the majority group being oils and the dominant compound content being propanoic acid (32.15%) at a retention time of 2.366 min.

Molecular docking assay

The potential of chemicals in *C. rotundicauda* as triple antiviral inhibitors for COVID-19 was assessed using molecular docking analysis using VinaWizard in the PyRx program. The proteins employed in this investigation comprised ACE2 (PDB ID: 7VX5) [18], RdRp (PDB ID: 7DFG) [19], and dan $3CL^{pro}$ (PDB ID: 7WYP) [20]. The results of the molecular docking analysis in Table 2 show that one compound has a better binding affinity value than the three control drugs synergistically, namely 2-methyl-5-(4′-methylphenyl)sulfonyl-4-nitroimidazole with a binding affinity for ACE2 (−7.0 kcal/mol); RdRp

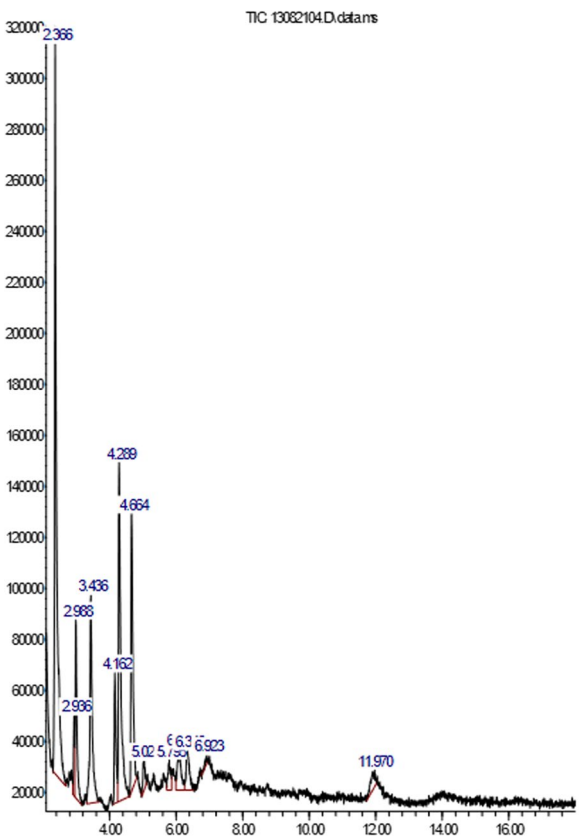

Fig. 1 GC–MS chromatogram of *C. rotundicauda* ethyl acetate extract. The peaks that appear are analyzed using an MS detector so that the name of the compound appears in Table 1. The peak with the highest concentration is peak number 1, namely propanoic acid

Table 1 Identification bioactive compound of *C. rotundicauda* ethyl acetate extract

Peak	RT (minute)	Composition (%)	Compound name
1	2366	32.15	Propanoic acid
2	2936	1.95	Toluene
3	2988	6.86	1,1,2-trichloroethane
4	3436	11.46	Butyl acetate
5	4162	4.93	Ethyl benzene
6	4289	17,99	*p*-xylene
7	4664	12.56	*o*-xylene
8	5025	1.48	1,1,2,2-tetrachloroethane
9	5795	1.78	2-methyl-5-(4′-methylphenyl) sulfonyl-4-nitroimidazole
10	6089	3.59	Octamethylcyclotetrasiloxane
11	6346	3.11	1,2,4-trimethylbenzene
12	6923	0.33	Dodecamethylcyclohexasiloxane
13	11,970	1.82	Azulene

Table 2 Binding affinity of *C. rotundicauda* bioactive compound

No	Compound	Binding affinity (kcal/mol)		
		ACE2	RdRp	$3CL^{pro}$
1	Chloroquine (control drug)	−5.8	–	–
2	Favipiravir (control drug)	–	−5.1	–
3	Boceprevir (control drug)	–	–	−6.7
4	Propanoic acid	−3.3	−3.3	−3.4
5	Toluene	−4.3	−3.9	−4.2
6	1,1,2-trichloroethane	−2.9	−2.9	−2.6
7	Butyl acetate	−3.8	−3.9	−3.5
8	Ethyl benzene	−4.5	−4.3	−4.3
9	*p*-xylene	−4.6	−4.3	−4.5
10	*o*-xylene	−4.5	−4.2	−4.3
11	1,1,2,2-tetrachloroethane	−3.3	−3.0	−2.7
12	2-methyl-5-(4′-methylphenyl) sulfonyl-4-nitroimidazole	−7.0	−5.9	−6.8
13	1,2,4-trimethylbenzene	−5.1	−4.8	−4.6
14	Azulene	−5.4	−5.0	−5.2

(−5.9 kcal/mol); and $3CL^{pro}$ (−6.8 kcal/mol). The binding affinity refers to the Gibbs free energy that arises from the interaction between a ligand and a receptor. A more negative or lower value of the binding affinity indicates a stronger binding affinity [21, 22]. The lower the binding affinity value of a complex, the more stable the complex formed and the more optimal its inhibitory activity [23, 24].

The position and type of interaction generated between the ligand and receptor are determined by visualizing potential compounds using Discovery Studio. The visualization results of 2-methyl-5-(4′-methylphenyl) sulfonyl-4-nitroimidazole are shown in Fig. 2a (ACE2), Fig. 2b (RdRp), Fig. 2c ($3CL^{pro}$), and Fig. 3 (3D visualization on active site). Various sorts of interactions can be formed by receptor–ligand complexes. Hydrogen bonds are bonds formed between H atoms and atoms with high electronegativities (F, O, and N) between amino acid residues and ligands [25]. Hydrophobic bonds are bonds between the hydrophobic groups of the ligand–receptor [26]. Electrostatic bonds are bonds formed due to the presence of a charge [27]. The ACE2 receptor with 2-methyl-5-(4′-methylphenyl)sulfonyl-4-nitroimidazole has similarities with the drug chloroquine with residue control positions Phe 390, Arg 393, Phe 40, Leu 73, and Leu 391. The drug control exhibits a hydrophobic bond at residues Phe 390 and Arg 393, while the prospective compound forms a hydrogen bond (and a hydrophobic bond at Phe 390). Notably, the strength of the hydrogen bond surpasses that of the hydrophobic bond. RdRp receptors with the potential compound 2-methyl-5-(4′-methylphenyl)sulfonyl-4-nitroimidazole have the same amino acid residue position as the drug favipiravir in position Val 560 (hydrogen bond) and Ala 512 (hydrophobic bond). Also, the $3CL^{pro}$ receptor with 2-methyl-5-(4′-methylphenyl)sulfonyl-4-nitroimidazole has similarities with the control drug boceprevir at Cys 145, Gly 143, Ser 144, Glu 166, and Leu 141 positions. The Cys 145 location of the drug control exhibits hydrogen and hydrophobic bond interactions, whereas in the prospective compound, only hydrophobic bonds are observed. At the Leu 141 position, distinct sorts of bonding are seen. Specifically, a hydrophobic link is formed in the control, but a hydrogen bond is created in the potential compound. In other residues, hydrogen bonds are also produced as a result of the same type of interaction. The similarity of these amino acid residues supports validation that the potential compound has a comfortable inhibitory position with the control drug. The similarity of these residues supports that the potential compounds have a similar inhibitory activity to the control drug compounds [28].

Pharmacokinetic ADME analysis

ADME pharmacokinetic analysis (absorption, distribution, metabolism, excretion) was performed on a potential compound, namely 2-methyl-5-(4′-methylphenyl) sulfonyl-4-nitroimidazole. The ADME profile of prospective compounds was determined by the utilization of the SWISSADME web server in this investigation [29]. The assessment of the ADME profile is advantageous in forecasting the efficacy of a pharmaceutical candidate upon its introduction into the organism [30, 31]. The results of the ADME analysis are given in Table 3. The potency

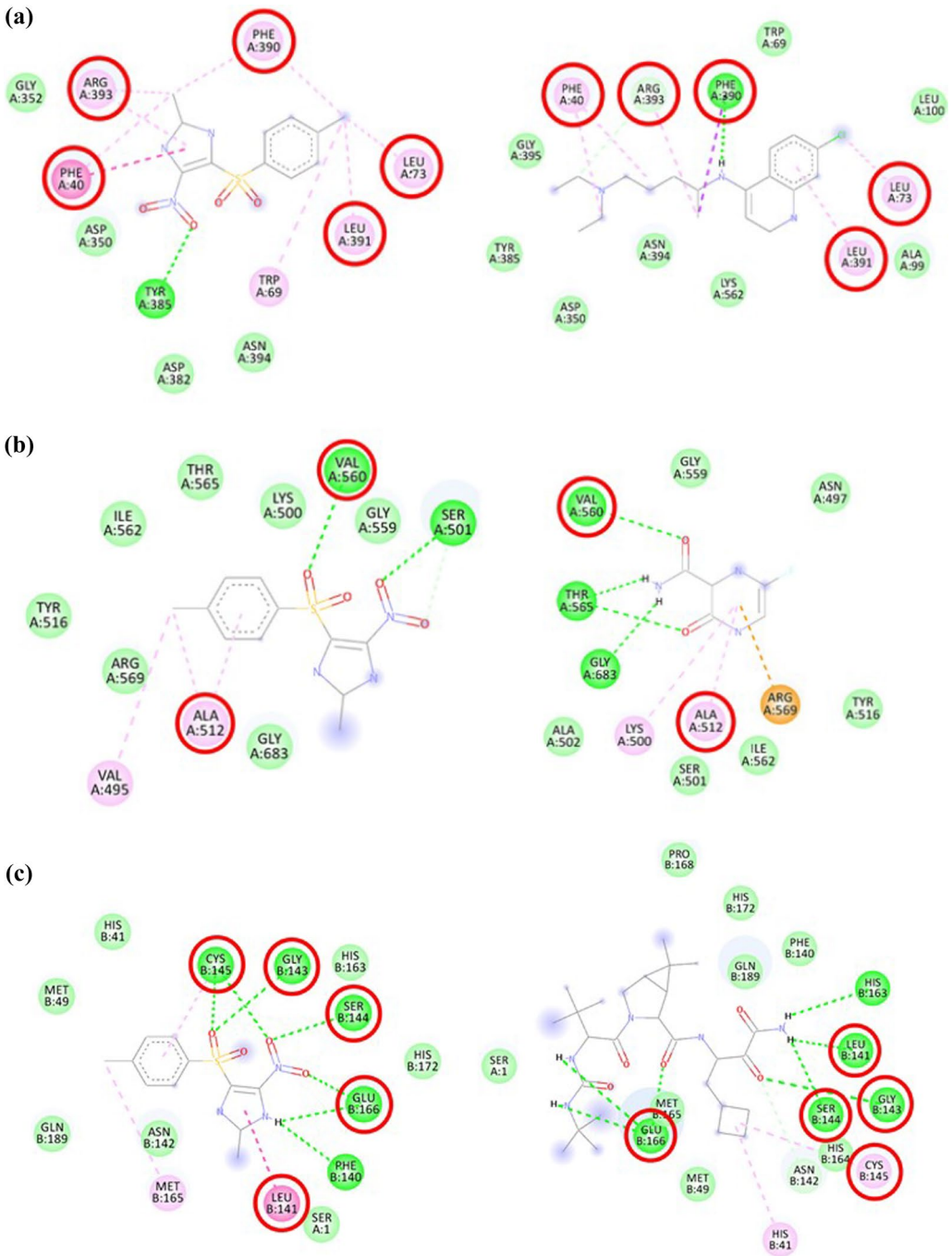

Fig. 2 **a** Interaction of potential and drug compound with ACE2. The red circle indicates the amino acid residues that are similar to the control. The red circle indicates amino acid residues that are similar to the control including Phe 390, Arg 393, Phe 40, Leu 73, and Leu 391. The interactions with the dotted line include hydrogen bonds (green) and hydrophobic bonds (pink). An interaction without a dotted line is a Van der Waals force interaction. **b** Interaction of potential and drug compound with RdRp. The red circle indicates the amino acid residues that are similar to the control. The red circle indicates amino acid residues that are similar to the control including Val 560 and Ala 512. The interactions with the dotted line include hydrogen bonds (green), electrostatic bond (orange), and hydrophobic bonds (pink). An interaction without a dotted line is a Van der Waals force interaction. **c** Interaction of potential and drug compound with $3CL^{pro}$. The red circle indicates the amino acid residues that are similar to the control. The red circle indicates amino acid residues that are similar to the control including Cys 145, Gly 143, Ser 144, Glu 166, and Leu 141. The interactions with the dotted line include hydrogen bonds (green) and hydrophobic bonds (pink). An interaction without a dotted line is a Van der Waals force interaction

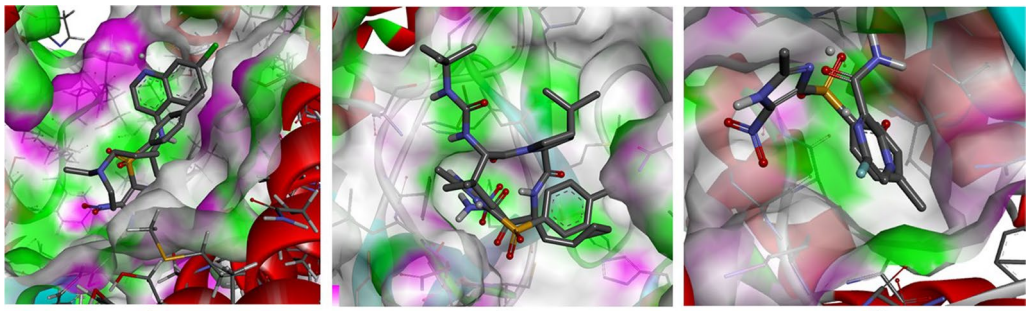

Fig. 3 3D interaction (surface area interaction) between ligand–receptor. **A** ACE2; **B** RdRp; **C** $3CL^{pro}$. The interaction surface area represents when the ligand is at its active site where the receptor in purple tends to be a hydrogen bond donor, while green tends to be a hydrogen bond acceptor

Table 3 Pharmacokinetics ADME of potential compound

Parameter	Score
Molar mass	281
Hydrogen bond donor	1
Hydrogen bond acceptor	5
Log P (lipophilicity)	5.848
Molar refractivity	66.654
Druglikeness lipinski	Yes
Bioavailability score	0.55
GI absorption	High
BBB permeability	No
P-gp substrate	No
CYP1A2 inhibitor	No
CYP2C19 inhibitor	No
CYP2C9 inhibitor	No
CYP2D6 inhibitor	No
CYP3A inhibitor	No
Log K_p (cm/s)	− 6.51

of the compound 2-methyl-5-(4′-methylphenyl)sulfonyl-4-nitroimidazole has compatibility with Lipinski's druglikeness parameter, which is a selection rule based on the five Lipinski rules that include molar mass ≤ 500 kDa, hydrogen bond donors ≤ 5, hydrogen bond acceptors ≤ 10, lipophilicity (log P) ≤ 5, and molar refraction 40–130 [32].

Discussion

C. rotundicauda is an animal that has the potential to be developed in the medical world, seeing that other species have been used. Research on the alleged content of these compounds in animals has not been reported in detail. This study aims to identify the compound content in the meat using ethyl acetate solvent. Ethyl acetate is a semipolar solvent that has the ability to attract polar and non-polar compounds so that compounds can be identified properly [33]. GC–MS is a method for identifying the content of compounds, especially volatile compounds (oils), in a matrix. The method begins with the separation of compounds by GC (gas chromatography) and identification by MS (mass spectrophotometer) [34]. The compounds that have been identified are then analyzed to determine their potential as COVID-19 antivirals using molecular docking.

The results of molecular docking found a compound that synergistically inhibits $3CL^{pro}$, RdRp, and ACE2. Visualization shows that these compounds form various kinds of interactions, namely hydrogen bonds, hydrophobic bonds, and electrostatic bonds. In addition, it was found that the complex did not form unfavorable bonds where a good complex was a complex that had few unfavorable bonds [26, 35]. In addition to the aforementioned, there exists a form of weak interaction known as the Van der Waals force, which arises from the interplay of atoms and is contingent upon the distance between them, hence determining the magnitude of this force. The congruence between the position or amino acid residues involved in the interaction of the proposed compound and the control indicates that the potential compound exhibits inhibitory characteristics similar to the pharmacological control [36]. The degree of similarity between the inhibitory location in the active site and the pharmacological control is directly proportional to the proposed compound's inhibitory action. The present work focused on the inhibition of ACE2, which serves as the entry route for the SARS-CoV-2 virus, as well as the inhibition of RdRp and $3CL^{pro}$ enzymes derived from SARS-CoV-2. These enzymes are known to play a crucial part in the replication phase of the virus. The docking results indicate that the potential compound exhibits synergistic potential in inhibiting three proteins. However, the binding affinity value suggests that the potential compound

demonstrates greater stability in inhibiting ACE2 compared to the other proteins. This is evident from the more negative binding affinity value associated with ACE2.

Lipinski's rule of five (Ro5) is a rule based on algorithmic rules that helps in the process of predicting drug potency. Pharmacokinetic analysis shows that the potential compounds have high gastrointestinal absorption, where this parameter is used to predict the absorption ability of drug candidates [37]. This result shows that the drug can be adequately absorbed in the intestine. In addition, the high bioavailability value of 0.55 indicates that this compound is suitable for oral consumption because it can be absorbed well by the body. [38]. In addition, there is no ability to bridge blood–brain barrier (BBB), so it can be considered to suppress lower side effects in the central nervous region. The BBB is a physiological barrier consisting of a layer of brain microvascular endothelial cells that separates it from the bloodstream [39].

Potential compounds also do not have potential as substrates of P-glycoprotein (P-gp substrate). P-gp is a protein that calcifies foreign substances out of cells widely distributed in the intestinal epithelium, stopping xenobiotics from returning to the intestinal lumen. [40]. P-gp plays a vital role in the absorption and excretion of the drug compound, so when a compound is a substrate of P-gp, it will be pumped out [41]. In addition, the potential compounds are predicted not to have inhibitory activity against all cytochrome P450 (CYP) isoforms. This result shows that this compound will be metabolized and excreted quickly from the body. Inhibition of isoforms of these enzyme systems by drugs can result in poor elimination and drug-induced toxicity. [42]. In addition, when a compound does not inhibit the activity of the CYP450 enzyme, it is likely that the potential compound will be easily transformed and can be taken orally [43].

Conclusions

This study examined the potential of the *C. rotundicauda* compound as an antiviral for SARS-CoV-2 through a triple inhibition mechanism through inhibition of ACE2, RdRp, and $3CL^{pro}$; it was found that there was one potential compound, namely 2-methyl-5-(4′-methylphenyl)sulfonyl-4-nitroimidazole, which has better binding affinity than the control drug and has a good ADME profile as a drug compound.

Methods

Sample preparation and extraction

The sample was split and separated for the flesh, visceral organs, gills, and carapace. The meat parts were taken and then macerated using ethyl acetate with a ratio of 1:3 (w/v) for 1 × 24 h. After maceration, the samples were separated by filtering and evaporated using a rotary evaporator to obtain a thick extract.

GC–MS analysis

The obtained extracts were tested by gas chromatography–mass spectrometry (GC–MS) to identify the compounds in Mimi Mintuna meat. Analysis used an Agilent 8890 GC with an Agilent 19091S-433UI column (dimensional 30 m × 250 μm × 0.25 μm). The sample was heated at 60–325 °C with a temperature increase of 100 °C/minute and left for 18 min. Helium gas was used as the carrier at a 1 mL/min flow rate. The injector was heated to 280 °C, and the sample was carefully maintained (1 μL injection size), with a split ratio of 1:10. There were the interactions between MS and ion sources at 280 °C and 150 °C. The mass spectrum of the *C. rotundicauda* bioactive compound was obtained at 70 eV within a reading range of 200–700 amu. The data obtained were analyzed with GC–MS software with NIST and Willey Library.

Molecular docking assay

The 3D conformer of the identified compounds and drug controls was obtained via the PubChem web server, which was minimized using OpenBabel in the PyRx software to convert the.sdf file to.pdb which aims to obtain a flexible conformer structure [44]. Proteins obtained by the RCSB webserver were sterilized using PyMOL and Discovery Studio to determine the active site [45], and the sterilized protein was then docked using Vina Wizard by PyRx [46]. The proteins used include ACE2 (PDB ID: 7VX5) (*X*: 161.262000; *Y*: 204.724875; *Z*: 284.353208) [18], RdRp (PDB ID: 7DFG) (*X*: 128.933609; *Y*: 131.912522; *Z*: 140.694652) [19], and $3CL^{pro}$ (PDB ID: 7WYP) (*X*: 15.349000; *Y*: −13.021278; *Z*: 1.423000) [20]. Then, visualization was performed with Discovery Studio to obtain types and positions of formed interaction.

Pharmacokinetics ADME analysis

Analysis of ADME (absorption, distribution, metabolism, and excretion) was performed by the SWISSADME web server [29]. ADME parameters include Lipinski's drug-likeness rule, bioavailability, GI absorption, BBB permeability, P-gp substrate, CYP inhibitor, and skin permeation [47].

Abbreviations

$3CL^{pro}$	3C-like protease
ACE2	Angiotensin-converting enzyme 2
ADME	Absorption, distribution, metabolism, excretion
BBB permeability	Blood–brain barrier permeability
CYP	Cytochrome
GC–MS	Gas chromatography–mass spectrometry
GI absorption	Gastrointestinal absorption
P-gp substrate	P-glycoprotein substrate
RdRp	RNA-dependent RNA polymerase

RNA	Ribonucleic acid
Ro5	Lipinski's rule of five
SARS	Severe acute respiratory syndrome
SARS-CoV-2	Severe acute respiratory syndrome coronavirus 2

Acknowledgements
The author thanks Belmawa for providing funding and Unesa for assisting in research.

Author contributions
MF and MS carried out the sample collection. AMS and EAV carried out the extraction and GC–MS analysis. AMS, DAR, and MKR carried out the analysis and wrote the manuscript. All authors read and approved the final manuscript.

Funding
This work was supported by Belmawa and Unesa.

Availability of data and materials
All datasets generated and analyzed during this study are available from the corresponding author on reasonable request.

Declarations

Ethics approval and consent to participate
Not applicable.

Consent for publication
Not applicable.

Competing interests
The authors declare that they have no competing interests.

Received: 9 June 2023 Accepted: 23 November 2023
Published online: 11 December 2023

References

1. Smith DR, Brockmann HJ, Beekey MA, King TL, Millard MJ, Zaldívar-Rae J (2017) Conservation status of the American horseshoe crab, (*Limulus polyphemus*): a regional assessment. Rev Fish Biol Fish 27(1):135–175. https://doi.org/10.1007/s11160-016-9461-y
2. World Conservation Monitoring Centre (1996) *Tachypleus gigas*. IUCN Red List Threat Species 1996:e(T21308A9266907):. https://doi.org/10.2305/IUCN.UK.1996.RLTS.T21308A9266907.en
3. Cartwright-Taylor L, von Bing Y, Chi HC, Tee LS (2011) Distribution and abundance of horseshoe crabs *Tachypleus gigas* and *Carcinoscorpius rotundicauda* around the main island of Singapore. Aquat Biol. https://doi.org/10.3354/ab00346
4. Chatterji A, Rathod V, Parulekar AH (1992) Spawning migration of the horseshoe crab, *Tachypleus gigas* (Muller), in relation to lunal cycle
5. Shin PKS, Li H, Cheung SG (2009) Horseshoe crabs in Hong Kong: current population status and human exploitation. In: Biology and conservation of horseshoe crabs. Springer, pp 347–360
6. Zimmermann H, Hewlett G, Rübsamen-Waigmann H (2009) Other inhibitors of viral enzymes and functions. Handb Exp Pharmacol 189(189):155–176. https://doi.org/10.1007/978-3-540-79086-0_6
7. Faizah M, Savita M, Vebianawati EA, Sururi AM, Rahayu DA (2022) Potensi dan persepsi masyarakat terhadap keberadaan Mimi Mintuna (horsheshoe crab) Di Pantai Batah Timur, Madura. In: Seminar Nasional IP2B V 2021
8. Funkhouser D (2011) Crab love nest. Sci Am 304(4):29
9. Ibrahim N, Ponnuraj KT, Ahmad A, Mokhtar KI (2019) Potential applications of horseshoe crab in biomedical research. J Biomed Clin Sci 4(2):12–18
10. Murakami T, Niwa M, Tokunaga F, Miyata T, Iwanaga S (1991) Direct virus inactivation of tachyplesin I and its isopeptides from horseshoe crab hemocytes. Chemotherapy 37(5):327–334. https://doi.org/10.1159/000238875
11. Ning Asih EN, Kawaroe M, Bengen DG (2018) Biomaterial compounds and bioactivity of horseshoe crab *Carsinoscorpius rotundicauda* biomass harvested from the Madura Strait. IOP Conf Ser Earth Environ Sci 141:012004. https://doi.org/10.1088/1755-1315/141/1/012004
12. Zimmer AJ, Klinton JS, Oga-Omenka C, Heitkamp P, Nawina Nyirenda C, Furin J, Pai M (2022) Tuberculosis in times of COVID-19. J Epidemiol Community Health 76(3):310–316. https://doi.org/10.1136/jech-2021-217529
13. Zhou P, Yang X-L, Wang X-G, Hu B, Zhang L, Zhang W, Si H-R, Zhu Y, Li B, Huang C-L, Chen H-D, Chen J, Luo Y, Guo H, Jiang R-D, Liu M-Q, Chen Y, Shen X-R, Wang X, Zheng X-S, Zhao K, Chen Q-J, Deng F, Liu L-L, Yan B, Zhan F-X, Wang Y-Y, Xiao G-F, Shi Z-L (2020) A pneumonia outbreak associated with a new coronavirus of probable bat origin. Nature 579(7798):270–273. https://doi.org/10.1038/s41586-020-2012-7
14. Geng R, Zhou P (2021) Severe acute respiratory syndrome (SARS) related coronavirus in bats. Anim Dis 1(1):4. https://doi.org/10.1186/s44149-021-00004-w
15. Sigrist CJ, Bridge A, Le Mercier P (2020) A potential role for integrins in host cell entry by SARS-CoV-2. Antiviral Res 177:104759. https://doi.org/10.1016/j.antiviral.2020.104759
16. Ahmad B, Batool M, Ain QU, Kim MS, Choi S (2021) Exploring the binding mechanism of PF-07321332 SARS-CoV-2 protease inhibitor through molecular dynamics and binding free energy simulations. Int J Mol Sci 22:9124
17. Huang J, Song W, Huang H, Sun Q (2020) Pharmacological therapeutics targeting RNA-dependent RNA polymerase, proteinase and spike protein: from mechanistic studies to clinical trials for COVID-19. J Clin Med 9(4):1131. https://doi.org/10.3390/jcm9041131
18. Wang Y, Xu C, Wang Y, Hong Q, Zhang C, Li Z, Xu S, Zuo Q, Liu C, Huang Z, Cong Y (2021) Conformational dynamics of the Beta and Kappa SARS-CoV-2 spike proteins and their complexes with ACE2 receptor revealed by cryo-EM. Nat Commun 12(1):1–13. https://doi.org/10.1038/s41467-021-27350-0
19. Yin W, Luan X, Li Z, Xie Y, Zhou Z, Liu J, Gao M, Wang X, Zhou F, Wang Q, Wang Q, Shen D, Zhang Y, Tian G, Aisa HA, Hu T, Wei D, Jiang Y, Xiao G, Jiang H, Zhang L, Yu X, Shen J, Zhang S, Xu HE (2020) Structural basis for repurpose and design of nucleoside drugs for treating COVID-19. bioRxiv. https://doi.org/10.1101/2020.11.01.363812
20. Qin B, Craven GB, Hou P, Chesti J, Lu X, Child ES, Morgan RML, Niu W, Zhao L, Armstrong A, Mann DJ, Cui S (2022) Acrylamide fragment inhibitors that induce unprecedented conformational distortions in enterovirus 71 3C and SARS-CoV-2 main protease. Acta Pharm Sin B 12(10):3924–3933. https://doi.org/10.1016/j.apsb.2022.06.002
21. Ralte L, Khiangte L, Thangjam NM, Kumar A, Singh YT (2022) GC–MS and molecular docking analyses of phytochemicals from the underutilized plant, *Parkia timoriana* revealed candidate anti-cancerous and anti-inflammatory agents. Sci Rep 12(1):1–21. https://doi.org/10.1038/s41598-022-07320-2
22. Saravanan R, Raja K, Shanthi D (2022) GC-MS analysis, molecular docking and pharmacokinetic properties of phytocompounds from *Solanum torvum* unripe fruits and its effect on breast cancer target protein. Appl Biochem Biotechnol 194(1):529–555. https://doi.org/10.1007/s12010-021-03698-3
23. Li J-X, Wang Y, Hao Y, Huo X-K, Sun C-P, Zhao X-X, Wang J-C, Zhang J-B, Ning J, Tian X-G, Wang C, Zhao W-Y, Lv X, Li Y-C, Ma X-C (2022) Identification of *Escherichia coli* β-glucuronidase inhibitors from *Polygonum cuspidatum* Siebold & Zucc. Braz J Pharm Sci. https://doi.org/10.1590/s2175-97902022e21394
24. Muhamed Ahmed A, Niazi ZR, Hanif M, Rafey A, Iqbal K, Pieters L, Amin A (2022) Computational analysis and in vitro investigation on citrus flavonoids for inflammatory, diabetic and AGEs targets. Braz J Pharm Sci. https://doi.org/10.1590/s2175-97902022e201056
25. Głowacki ED, Irimia-Vladu M, Bauer S, Sariciftci NS (2013) Hydrogen-bonds in molecular solids—from biological systems to organic electronics. J Mater Chem B 1(31):3742–3753. https://doi.org/10.1039/C3TB20193G
26. Cheng X, Shkel IA, O'Connor K, Record MT (2020) Experimentally determined strengths of favorable and unfavorable interactions of amide atoms involved in protein self-assembly in water. Proc Natl Acad Sci 117(44):27339–27345. https://doi.org/10.1073/pnas.2012481117

27. Njoroge FG, Chen KX, Shih N-Y, Piwinski JJ (2008) Challenges in modern drug discovery: a case study of boceprevir, an HCV protease inhibitor for the treatment of hepatitis C virus infection. Acc Chem Res 41(1):50–59. https://doi.org/10.1021/ar700109k
28. Shifeng P, Boopathi V, Murugesan M, Mathiyalagan R, Ahn J, Xiaolin C, Yang D-U, Kwak G-Y, Kong BM, Yang D-C, Kang SC, Hao Z (2022) Molecular docking and dynamics simulation studies of ginsenosides with SARS-CoV-2 host and viral entry protein targets. Nat Prod Commun 17(11):1934578X221134331. https://doi.org/10.1177/1934578X221134331
29. Daina A, Michielin O, Zoete V (2017) SwissADME: a free web tool to evaluate pharmacokinetics, drug-likeness and medicinal chemistry friendliness of small molecules. Sci Rep 7(1):1–13
30. Obuotor TM, Kolawole AO, Apalowo OE, Akamo AJ (2023) Metabolic profiling, ADME pharmacokinetics, molecular docking studies and antibacterial potential of Phyllantus muellerianus leaves. Adv Tradit Med 23(2):427–442. https://doi.org/10.1007/s13596-021-00611-5
31. Sympli HD (2021) Estimation of drug-likeness properties of GC–MS separated bioactive compounds in rare medicinal *Pleione maculata* using molecular docking technique and SwissADME in silico tools. Springer, Vienna
32. Lipinski CA (2004) Lead- and drug-like compounds: the rule-of-five revolution. Drug Discov Today Technol 1(4):337–341. https://doi.org/10.1016/j.ddtec.2004.11.007
33. Rydberg J, Cox M, Musikas C, Choppin GR (2004) Solvent extraction principles and practice. Taylor & Francis
34. Hussain SZ, Maqbool K (2014) GC-MS: principle, technique and its application in food science. Int J Curr Sci 13:116–126
35. Sururi AM, Maharani DK, Wati FA (2023) POTENSI SENYAWA EUGENOL DARI CENGKEH (*Syzygium aromaticum*) SEBAGAI INHIBITOR PROTEASE HIV-1 (PR). Unesa J Chem 12(1):26–30
36. Nugroho ED, Ardiansyah R, Kurniawan N, Rahayu A, Sururi AM (2023) An in-silico study on the chemical compounds from macrophiothrix longipedia as antiviral compounds against COVID-19. 16(4):2380–2390
37. Pires DE V, Kaminskas LM, Ascher DB (2018) Prediction and optimization of pharmacokinetic and toxicity properties of the ligand. In: Computational drug discovery and design. Springer, pp 271–284
38. Martin YC (2005) A bioavailability score. J Med Chem 48(9):3164–3170. https://doi.org/10.1021/jm0492002
39. Lin J, Sahakian DC, De Morais SM, Xu JJ, Polzer RJ, Winter SM (2003) The role of absorption, distribution, metabolism, excretion and toxicity in drug discovery. Curr Top Med Chem 3(10):1125–1154
40. Finch A, Pillans P (2014) P-glycoprotein and its role in drug-drug interactions. Aust Prescr 37(4):137–139
41. Elmeliegy M, Vourvahis M, Guo C, Wang DD (2020) Effect of P-glycoprotein (P-gp) inducers on exposure of P-gp substrates: review of clinical drug–drug interaction studies. Clin Pharmacokinet 59:699–714
42. Ononamadu CJ, Ibrahim A (2021) Molecular docking and prediction of ADME/drug-likeness properties of potentially active antidiabetic compounds isolated from aqueous-methanol extracts of *Gymnema sylvestre* and *Combretum micranthum*. Biotechnol J Biotechnol Comput Biol Bionanotechnol 102(1):85–99
43. Srimai V, Ramesh M, Satya Parameshwar K, Parthasarathy T (2013) Computer-aided design of selective cytochrome P450 inhibitors and docking studies of alkyl resorcinol derivatives. Med Chem Res 22(11):5314–5323
44. Sururi AM, Raihan M, Aisa ER, Safitri FN, Constaty IC (2022) Anti-inflammatory activity of stem bark dichloromethane fraction *Syzygium samarangense* extract as COX-2 inhibitor: a bioinformatics approach. J Kim Ris 7(2):94–100. https://doi.org/10.20473/jkr.v7i2.39662
45. Kakkassery KR, Raphael JT, Johnson VP (2021) In vitro antibacterial and in silico docking studies of two Schiff bases on Staphylococcus aureus and its target proteins. Futur J Pharm Sci 7(1):78. https://doi.org/10.1186/s43094-021-00225-3
46. Trott O, Olson AJ (2010) AutoDock Vina: improving the speed and accuracy of docking with a new scoring function, efficient optimization, and multithreading. J Comput Chem 31(2):455–461. https://doi.org/10.1002/jcc.21334
47. Ullrich S, Nitsche C (2020) The SARS-CoV-2 main protease as drug target. Bioorg Med Chem Lett 30(17):127377. https://doi.org/10.1016/j.bmcl.2020.127377

Publisher's Note